Chapter 5. Results

5.1 Transverse mass spectra for pions, kaons and protons

Transverse mass spectra for identified pions, kaons and protons for both sulphur on sulphur collisions and lead on lead collisions at the central rapidity will be discussed in this section. Invariant cross sections $1/M_T\ dN/dM_T$, which was mentioned in the previous chapter, as a function of $M_T - mass$ will be shown in the figure for protons, kaons and pions from the top to the bottom in the figure 5-1, the left hand side of the figure is for Pb+Pb collisions and the right hand side is for S+S collisions. The contents described here will be focused on the shape of the distributions for the different particle species and the different colliding system. A fitting procedure to the each slope has been done with a single exponential function excluding the low P_T pions, which are well known as contaminated by resonance decaies. The fitted inverse slope parameter is seen on the top of each slope. Centralities for both systems are similar around top 15% of total geometrical cross section.

Points to be emphasized are the following. All transverse mass spectra for pions, kaons and protons for both colliding systems are well described with a single exponential function. The fitted inverse slope parameter increases with increasing the particle mass for both systems. The fitted inverse slope parameter for the same mass particle increases with increasing with the colliding system. The difference of the fitted inverse slope parameters between the colliding systems also increases with the particle mass.

The fitted inverse slope parameters are summarized in the figure 5-2 as a function of particle mass for each system. Proton on proton collisions data which is from ISR experiment [5-1] are added for the comparison. An increase of the inverse slope parameters with the particle mass, which had not seen in the p+p collisions, is clearly observed in the heavy-ion collisions. The data are fitted with the following formula as a function of mass.

$$T_m = T_f + C\beta_s^2 M,$$

where T_m is the measured slope parameter, T_f is a freeze-out temperature, β_s is a hydro-dynamical transverse surface flow velocity, M is a mass of the particle and C is a constant where we don't really know about this constant, but we here assume this constant is same for different colliding systems. Here we used $C = 0.4$ in the fitting procedure. The basic idea of this formula is that the measured inverse slope parameter is explained by two types of motion, one is random or thermal motion described by T_f, another is collective motion described by β_s. The increase of the slope parameter intuitively suggests an existence of the hydro-dynamical transverse flow of the colliding matter. An inclination of the fitted line increases with the size of the colliding system, where the inclination corresponds to the transverse flow velocity. Therefore an increase of the transverse flow velocity β_s with the colliding system is found to be $\beta_s = 0.0$ for p+p, $\beta_s = 0.4$ for S+S and $\beta_s = 0.5$ for

Pb+Pb collisions. An intersection of the fitted line of the inverse slope at mass=0 is corresponding to the freeze-out temperature T_f, which is found to be around 140 ± 15 (MeV). The results shown here suggest a scenario that secondary particles freeze out at the same temperature, and this freeze-out temperature does not increase with increasing the colliding system too much. This is a signal that a thermalization might be already achieved locally around the central rapidity region at SPS energy.

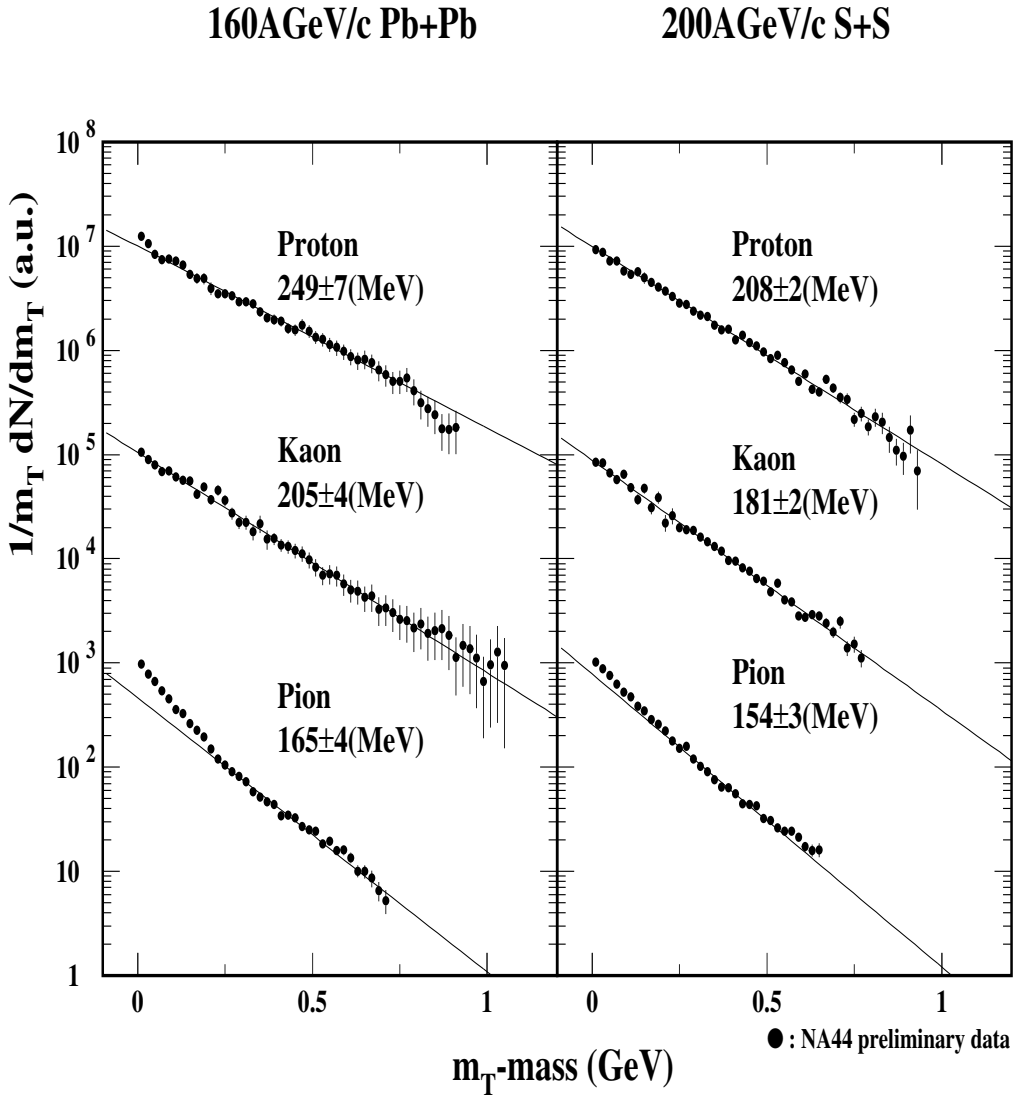

Figure 5-1: transverse mass spectra for hadrons

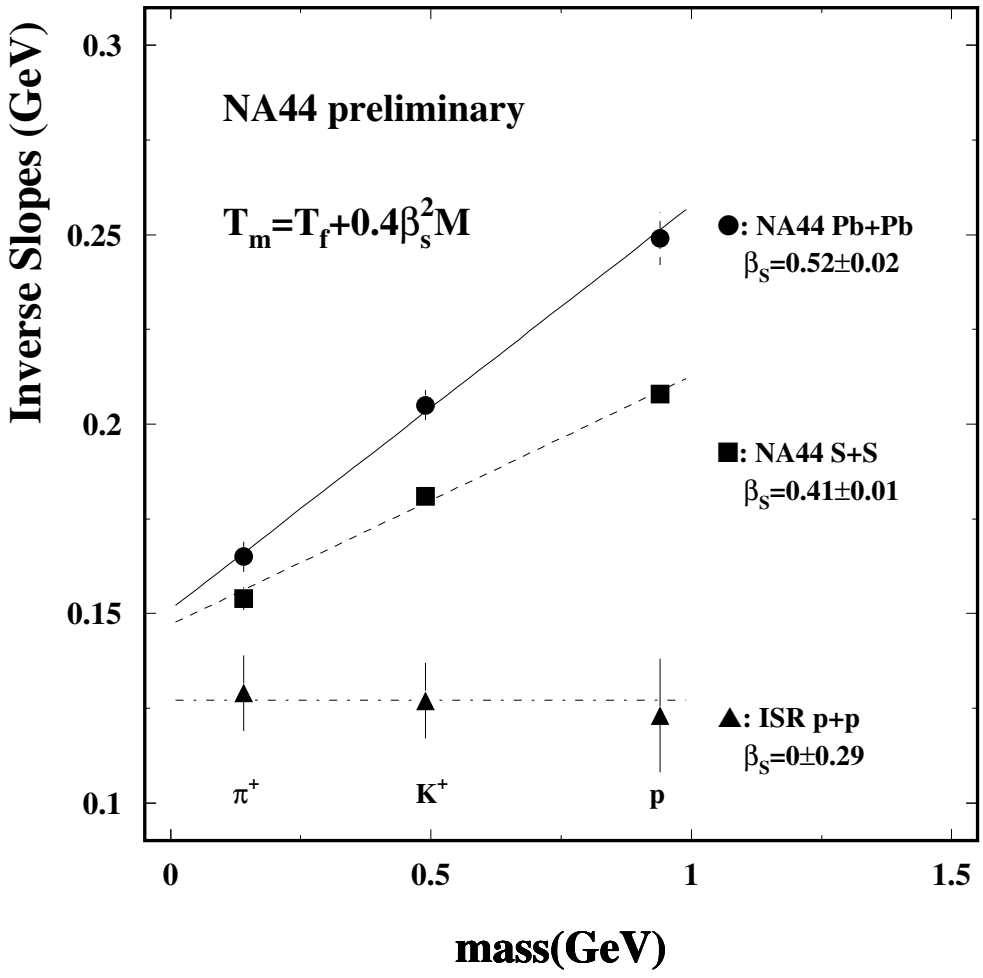

Figure 5-2: summary of inverse slope parameters

5.2 dN/dy for pion

By integrating the absolutely normalized invariant cross section over M_T, dN/dy for pion is calculated to be 12.4 $\pm$ 0.8 for S+S collision and 89.5 $\pm$ 9.5 for Pb+Pb collisions. Because pion M_T slopes are clearly curved, a single exponential function can not explain the spectrum. Therefore, for both systems, two exponential components are assumed. The fitting of two exponential functions is seen in the figure 5-3 and the fitted functions agree with the experimental spectra rather well. The shape of two distributions are similar, although the colliding system is completely different from S+S to Pb+Pb.

The difference of the total incident energy of the beam particle between 200 AGeV/c sulphur (6.4 TeV) and 160 AGeV/c lead (33 TeV) is 5.2 as a ratio of those two total energies. On the other hand, the ratio of measured dN/dy Pb+Pb over S+S is 7.2 $\pm$ 0.9, which is larger than the ratio of the two beam energies. dN/dy distributions of negatively charged particle measured at NA35/NA49 experiment for both 200 AGeV/c S+S and 160AGeV/c Pb+Pb at SPS are presented in the figure 5-4. The shape of the distribution does not change too much, the ratio Pb+Pb over S+S is around 8.2 $\pm$ 0.3 [5-2]. The difference of the absolute value of dN/dy between NA44 and NA35/NA49 may be caused by the difference of centrality and the difference of particle identification. Assuming a similar production between pion$^+$ and pion$^-$, the ratio of dN/dy as Pb+Pb over S+S measured in the both experiments are clearly larger than the ratio of these two beam energies. This increase may suggests an increase of the re-scattering during the collisions and a higher baryon stopping in Pb+Pb collisions and some degree of transparency in S+S collisions, which will be discussed in the following section. Those pion rapidity distributions are too broad to be purely thermal. Those data rule out thermal models which incorporate a spherically symmetric radial expansion, but but are consistent with hydro-dynamical models which assume primarily longitudinal expansion.

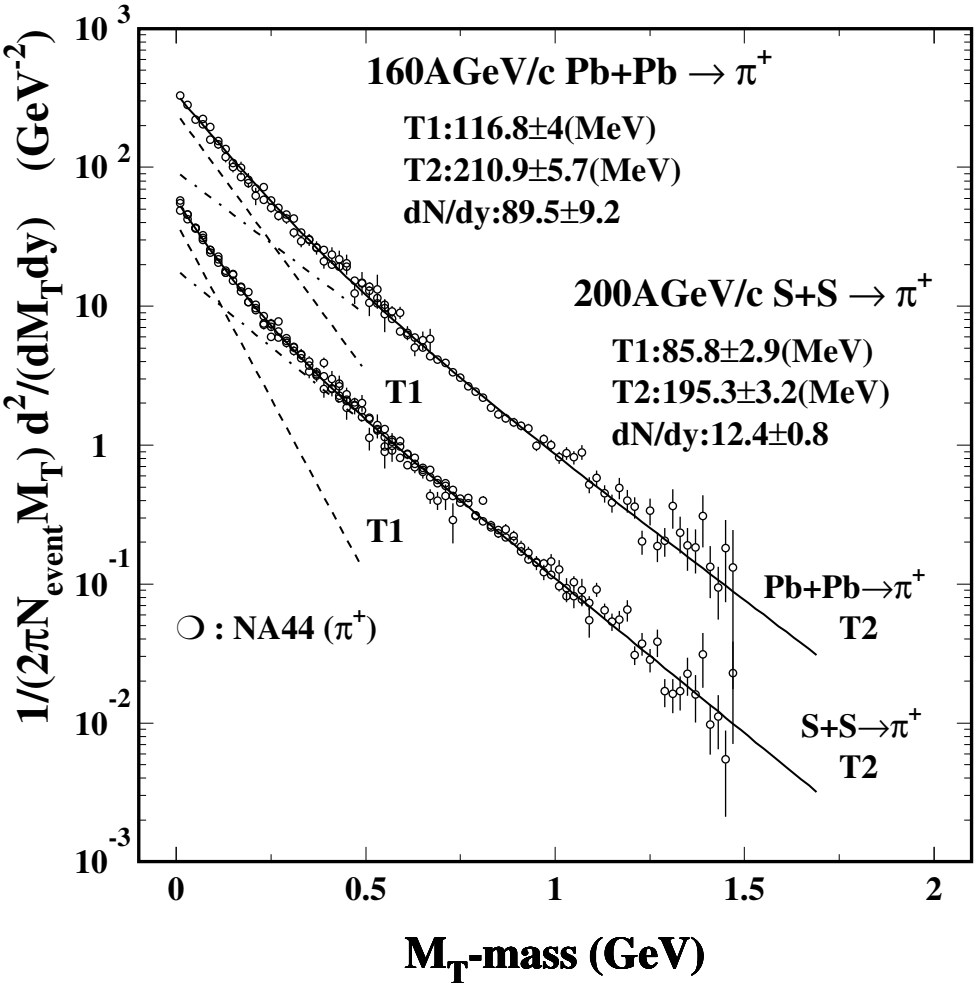

Figure 5-3: normalized invariant cross section for pion

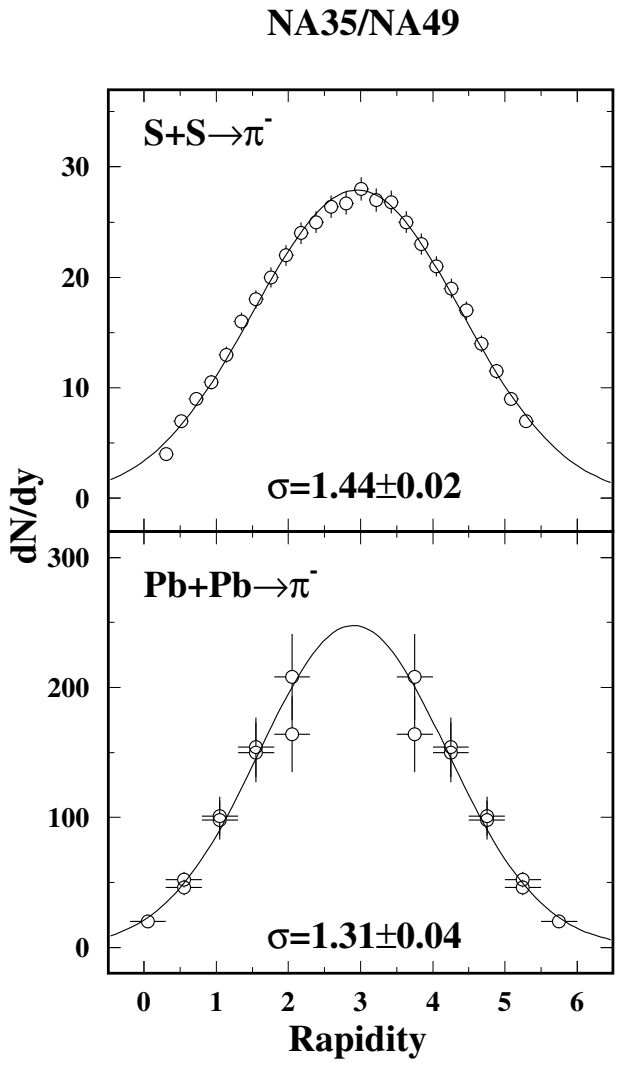

Figure 5-4: pion$^-$ dN/dy

5.3 Proton rapidity distributions

Proton rapidity distributions for sulphur on sulphur collisions and for lead on lead collisions will be presented in this section and shown in the figure 5-5. dN/dy's are calculated by integrating the absolutely normalized transverse momentum spectra with assuming single exponential shape, where this method was described in the previous chapter. These calculations were done at 8GeV/c and 4GeV/c momentum settings at horizontal spectrometer magnet configuration, the different momentum setting with NA44 spectrometer gives the another measurement at the different rapidity (smaller rapidity at the smaller momentum setting). Because of the collision symmetry for both S+S and Pb+Pb, two measured points dN/dy's are reflected around the central rapidity. Proton rapidity distribution is a strongest tool to measure the nuclear stopping power. Because of the baryon number conservation during the collisions, total number of the proton over the full phase space can not excess too much above the original proton number in the colliding two nuclei, since $N\overline{N}$ pair production is not big at this energy. By fixing the integrated number of proton over rapidity to be a constant at the original number of the colliding two nuclei, proton rapidity distribution can be used to measure the amount of the stopped proton at central rapidity in order to estimate the nuclear stopping power.

By comparing the shape of the two rapidity distributions for S+S and Pb+Pb, a flat plateau or U shape distribution around the central rapidity seen in the lighter ion collisions is changed into a center peaked distribution in the truly heavy-ion collisions. The first, a flat plateau rapidity distribution is already telling that the nuclear transparent picture is not completely right at this SPS energy, the nuclear stopping is already increasing in the S+S collisions. This phenomenon of the center peaked rapidity distribution is clearly saying that the higher nuclear stopping in achieved in the Pb+Pb collisions. This proves that the higher baryon density region is exist around the central rapidity.

The high baryon density may cause the large re-scattering between the produced particles, and thermalization of the system may achieved around the central rapidity. The results which has seen on the transverse momentum spectra of the secondary particles in the previous section is confirming this increase of the nuclear stopping power.

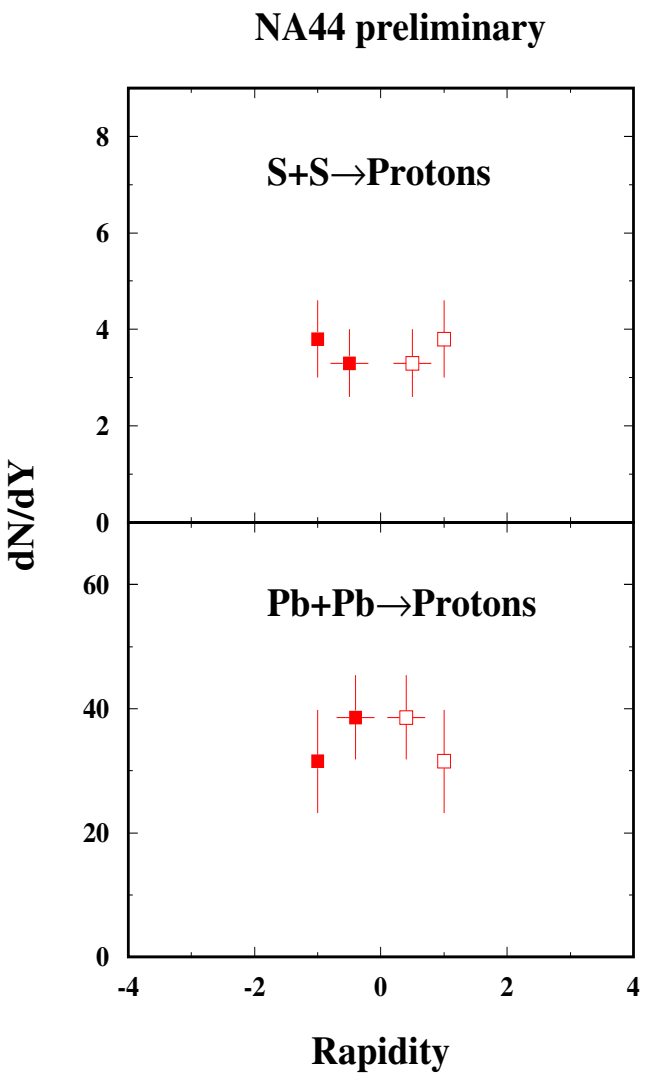

Figure 5-5: proton dN/dy

5.4 Two particle interferometry for pions and kaons

Two particle correlation functions for pions and kaons in sulphur on lead collisions around central rapidity are presented in this section. Two pion event samples are collected at two different transverse momentum regions, low P_T region ($0.0 < P_T < 0.4$) and high P_T region ($0.3 < P_T < 0.8$), which are corresponding to two different spectrometer angle settings, small angle setting (44 mrad) and large angle setting (131 mrad), they are taken both at the 4GeV/c spectrometer momentum setting. On the other hand, two kaon event samples are collected at the 6GeV/c small angle setting, covered transverse momentum range is ($0.0 < P_T < 0.6$). Data presented here are analyzed in two dimensionally in (Q_T,Q_L) in order to focus on the transverse size R_T of the emitting source of the identified particle. Because the data are taken at horizontal magnetic setting, transverse momentum difference Q_T is domained by Q_{TO}. Therefore the measured R_T is mainly influenced by R_{TO}, which is a combination of the transverse size and the time duration of the particle emitting source distribution.

Two dimensional chi-square contour maps are shown at the fixed λ having the lowest chi-square for each setting in the top three figures in the figure 5-6. Here the procedure to make these chi-square contour maps are explained in the previous chapter. Experimental correlation functions and Monte Carlo output correlation functions which have the smallest chi-square are shown on the top of each other for the comparison in the figure 5-6. Fully corrected two dimensional correlation functions in Q_T and Q_L and those projections can be seen in the next figure 5-7.

The similar transverse size R_T around 2-3 (fm) for both high P_T pions and low P_T kaons are observed, compared with the larger transverse size around 4 (fm) for low P_T pion. The larger size of low P_T pion can be explained by the resonances contribution ω, η and η' or other heavy resonances having a long life time. At higher P_T, those contribution to pion are estimated to be smaller than at lower P_T. Charged kaon are less affected by resonance decay than pions. The result is that pion and kaon source sizes in the resonance-less region are found to be comparable. This suggests pions and kaons are emitted from similar space region and time duration of the colliding system, which is consistent with the previously mentioned scenario that all hadrons are frozen-out at the same freeze-out temperature with the same velocity. This results add one more confidence to the freeze-out scenario, which is the same freeze-out volume for all hadrons.

On the other hand, there is another explanation to the resulting source sizes. A simple hydro-dynamical model, which predict the radius parameters to scale as $1/\sqrt{M_T}$ for all mesons. The collective expansion will create a strong position-momentum correlation in both longitudinal and transverse directions. The velocity gradient together with the freeze-out temperature generate a length scale in all three dimensions. If the source length scales are considerably larger than this, for a cylindrically symmetric three dimensional expansion, the measured radius parameters become equal in the LCMS system and will show $1/\sqrt{M_T}$ dependence [2-2]. In

the figure 5-8, the measured data are complied as a function of M_T, the solid line shows the fitted line with $A/\sqrt{M_T}$, where A is a fitting parameter. The data agree with this hydro-dynamical model fairly well, too. If this is right, the measured sizes are not representing the real source size, it's just kinematical effect which is coming from the position-momentum correlation caused by the radial and longitudinal expansion, however the $1/\sqrt{M_T}$ dependence also depends on the strength of the position-momentum correlation compared to the source extension.

One more consideration to the measured source size is the experimental acceptance. Because of the narrow momentum acceptance of the experiment and the position-momentum correlation of the expanding source, the experimental acceptance will directly define the size of the window or the aperture of our telescope, which is a tool called a two particle interferometry in this case. This means that two particle event samples are collected from the small fraction of the total particle-emitting source distribution, in another word, our telescope looks only small part of whole fire ball. In addition to this, the position-momentum correlation will reduce the measured source size even more, if one measures the source size with two particle interferometry technique. The reason is exist inside of the interferometry technique itself, an enhancement of detecting two identical particles which have two close momenta, in another word, which come from two close positions caused by the strong position-momentum correlation, will define the measured source size. In this sense, the interferometry technique is in principle not suitable to measure the size of the expanding source, which has the strong position-momentum correlation, since it is not chaotic source. To understand the expanding source and the interferometry, one needs to distinguish contributions into the measured source size from the geometrical size and the size made by the position-momentum correlation. Therefore, it is important to compare the measured data with model simulations. This will be discussed in the following chapter.

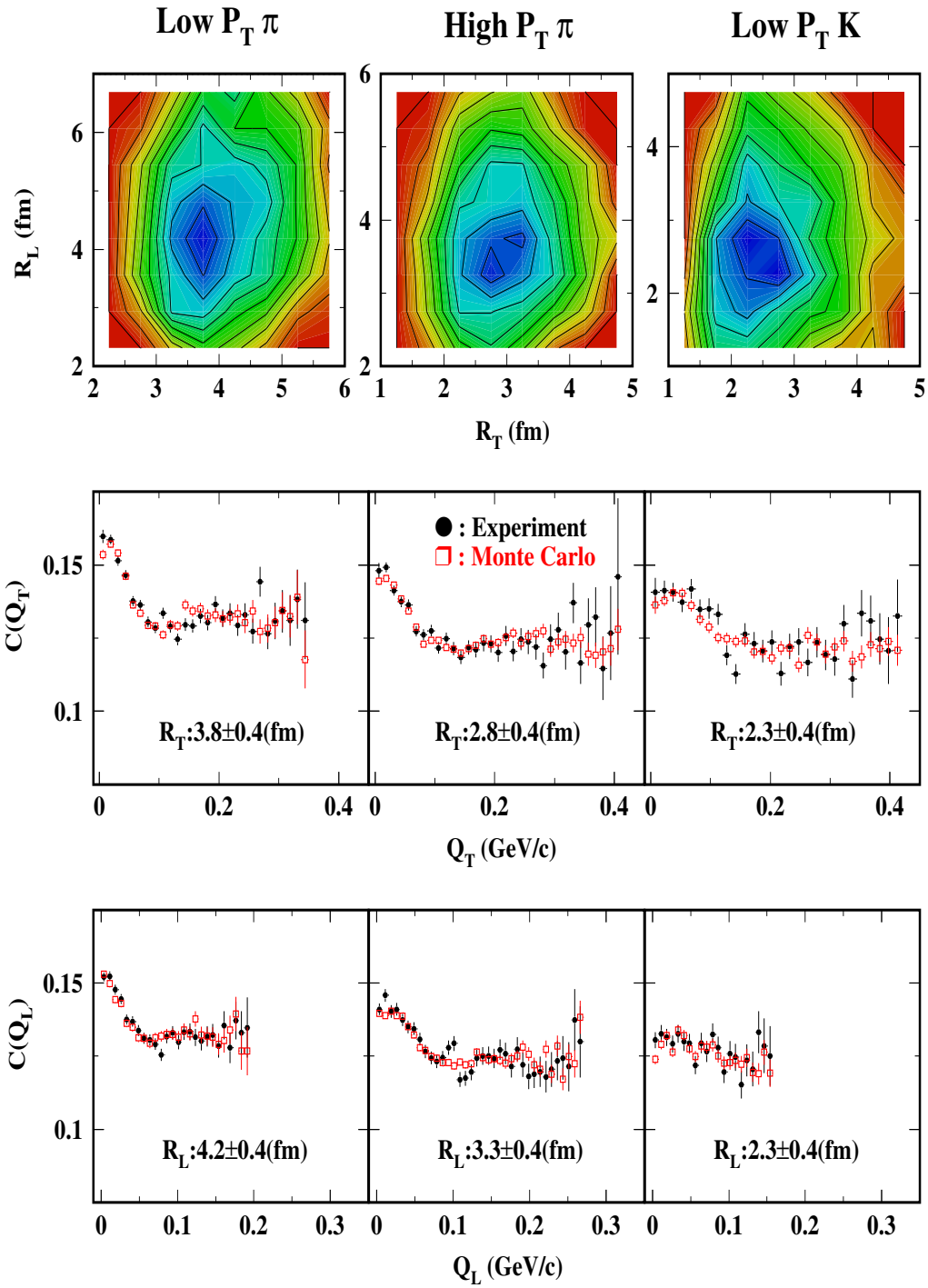

Figure 5-6: chi-square map and comparison with MC at the smallest chi-square

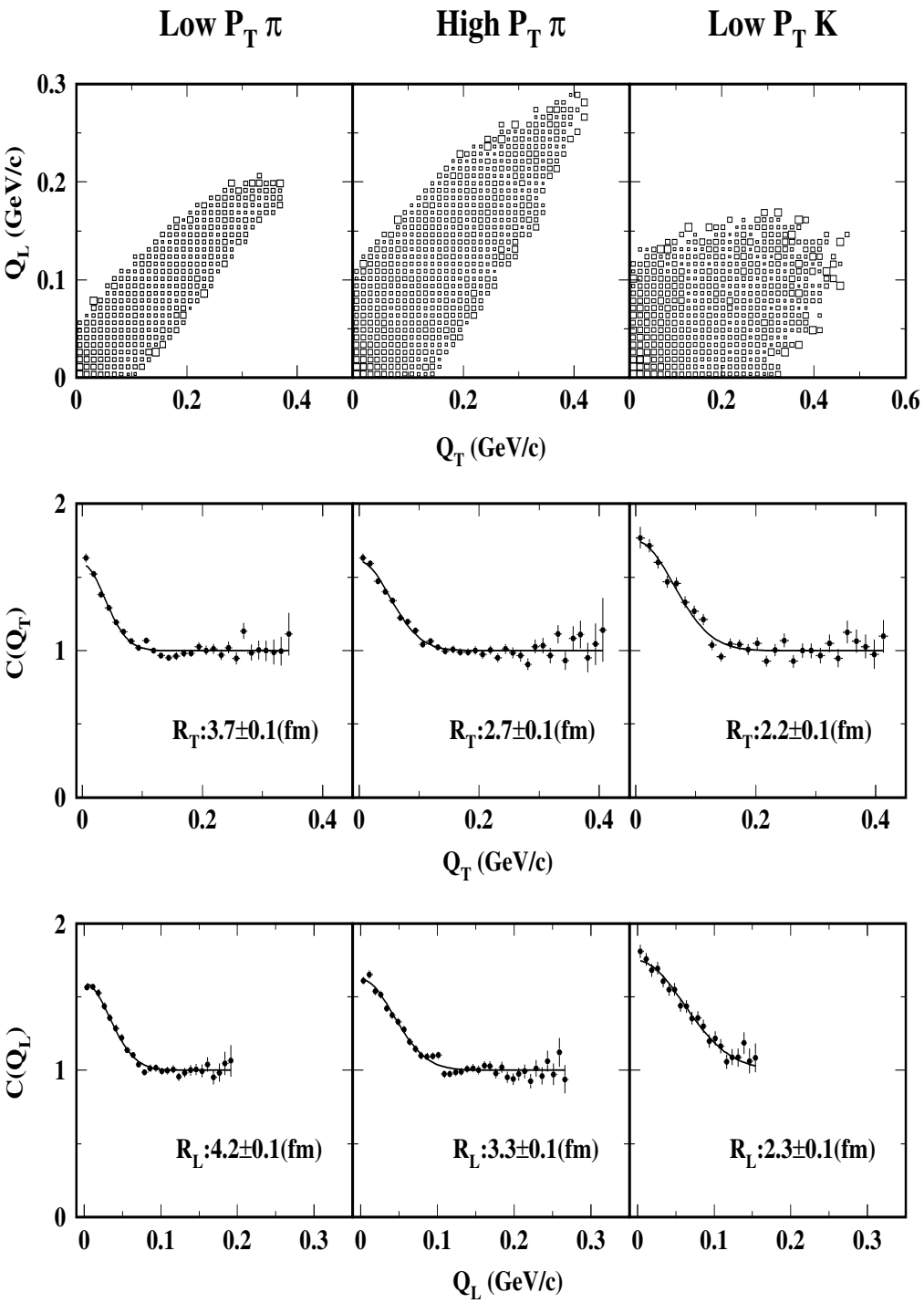

Figure 5-7: corrected two-dimensional correlation functions and projections

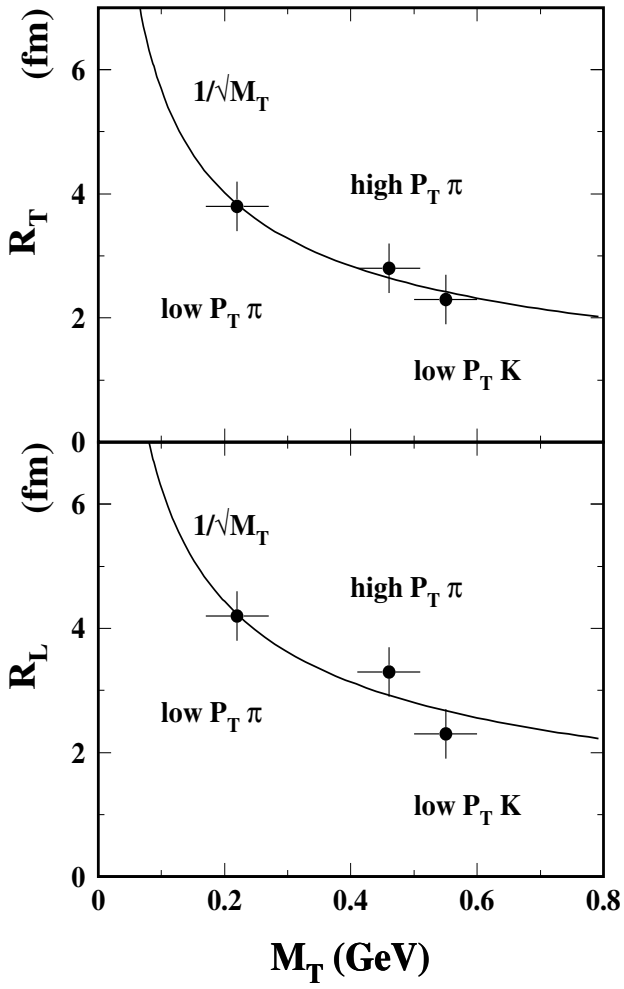

Figure 5-8: summary of measured radius parameters